Available online at www.sciencedirect.com

ScienceDirect

Procedia Computer Science 2 (2010) 272–282

Procedia Computer Science

www.elsevier.com/locate/procedia

ICEBT 2010

Microcalcification Detection in Digital Mammograms using Novel Filter bank

T.Balakumaran[a*], ILA.Vennila[b], C.Gowri Shankar[c]

[a] *Department of ECE, Coimbatore Institute of Technology, Coimbatore, India*
[b]*Department of EEE,PSG college of Technology, Coimbatore, India*
[c]*Department of EEE,Velalar college of Engineering and Technology, Erode, India*

Abstract

Mammography is a widely used diagnostic technique for early breast cancer detection in women. Clusters of Microcalcification are the sign of breast cancer and their detection will decrease the probability of mortality rate and improves its prognosis. The detection of microcalcification clusters is a difficult task for radiologists because of variations of size and orientation and are highly correlated with background tissue. In this paper, we present a Computer Aided Detection (CAD) method, which is used to detect nodules (microcalcification) in mammograms. We have designed a multi-scale filter bank based on the concept of second-order partial derivatives (Hessian matrix). Regions Of Interest (ROI) are identified by a multiresolution based histogram technique. This ROI of mammogram is decomposed into sub-bands, the low-frequency subband is suppressed and then the high-frequency subbands which contain only nodule-like structures are reconstructed. This structure is determined by the eigenvalues of the Hessian matrix. The detection performance of the proposed method is evaluated by comparing our results with two traditional wavelet based methods. Experimental results show that the microcalcifications can be efficiently detected by proposed method and it has high true positive ratio in comparison to other methods.

Keywors: Breast Cancer, Computer Aided Detection, Hessian matrix, two dimensional filter banks

1. Introduction

Breast cancer is the second leading cause of cancer deaths for women in the world with the highest mortality, causing 2,70,000 victims in every year. This high death rate results from the tedious to detect breast cancer in an early stage. A Most widely-used technique for breast cancer detection is the analysis of the Screening mammography [1]. Therefore, routine screening mammogram programs are considered as a possible option to detect the earlier sign of cancer. Earliest sign of breast cancer is microcalcification, which is nodular in structure and varies in dimension from 0.1 mm to 1 mm. A detection of microcalcification in such earlier stage increases the probability of surviving [2]. The microcalcification detection is a challenging task in medical imaging. There are many aggravating conditions which make the detection process more complex. The major difficulty is erratic shape of the microcalcification. They are approximately nodular, but the shape might be blob, elliptical and circular. Another one is the intensity variation of the calcification. The intensity varies exceptionally sharply compared to other tissue. These nodules are difficult to detect in mammogram and most of the nodules are missed by radiologists. The sensitivity of radiologists for microcalcification detection is 70 % - 90 % [3,4].

Therefore computerized output for breast cancer detection on mammogram has been developed. Computer Aided Detection (CAD) is vital to increase the accuracy of the detection process [5-9]. The regions which are detected by CAD system then be observed by a radiologist, who finally confirms those as true or false positives. So the goal of a CAD system is to increase the true positive rate and decrease the false positives.

In the past two decades a number of methods have been proposed for breast cancer detection. These methods are based on suppressing background information and amplifying suspicious areas. Normally microcalcification appears as group of tiny bright spots in the mammograms. These bright spots, correspond to high-frequency in the frequency spectrum. These high-

* Corresponding author. Tel.:+91-422-2432902
E-mail address:erbala12@yahoo.com

1877-0509
doi:10.1016/j.procs.2010.11.035

frequency features of an image can be recovered using the wavelet-based subband decomposition. Most of researchers have developed a method based on wavelet transform, which is a robust tool for image denoising, enhancement and image analysis [10], [11]. Wavelet transform is a powerful method for analyzing spatial-frequency phenomena and it allows the decomposition of image into different frequency bands without affecting the spatial locality.

Wang and Karayiannis [12], Strickland *et al. [13],* Yoshida *et al.* [14], [15] used a Discrete Wavelet Transform, D.Sersic et al [16] presented novel filter bank based on redundant wavelet transform, Laine *et al.* [17], [18] applied dyadic wavelet transform, Chun-Ming Chan et al [19] developed an algorithm relying on multiscale wavelet analysis for detection of microcalcification. In Their approach, mammogram was decomposed into different frequency subbands, the low frequency subband is suppressed and only the high frequency subbands are reconstructed. These high frequency subbands are enhanced by gain factors before reconstructing. The gain factors were determined by training, supervised learning and trial and error method. The resultant reconstructed image enhances not only microcalcification clusters but also some other structures, such as blood vessels and artifacts, which are high frequency in nature. So enhancing only the microcalcification clusters is a significant task in the reconstructed image. Extraction of microcalcification from high frequency subbands is done based the structure and size of the microcalcification clusters.

CAD system is developed to extract the objects based on structure and dimensions. In few papers, Hessian matrix is used to extract the different structures of object in medical imaging. Y.Sato *et al.* [20] used 3D Hessian matrix to classify the different structure of tissues in three-dimensional images. Frangi *et al.* [21] employed the Hessian matrix for vessel enhancement. Krissian *et al.* [22] developed a multi-scale detection in 3D images to detect the blood vessels. Krissian *et. al* [22], Frangi *et al.* [21] used multiscale detection based on eigenvalues of Hessian matrix for vessel detection. We modified their method for detection of microcalcification in mammogram. Nodular Structure can be is identified by eigenvalues of Hessian matrix and dimension can be identified by multiscale analysis. The eigenvalues of the Hessian matrix of all pixels are analyzed and identified if there is a local nodular structure present or not. The images were obtained by a high resolution screening mammogram. The aim of the proposed method is to achieve an early nodule detection of various dimensions. This method is also rotation-invariant. This assists to detect microcalcification with various size and arbitrary orientation.

The rest of the paper is organized as follows. Section 2 presents the microcalcification detection by proposed method. It includes ROI detection, novel filter bank design for nodular detection and proposed method. Section 3 presents a result and discussion and conclusion as last section.

2. Microcalcification Detection

An entire system of our proposed method for microcalcification detection in mammogram is composed of two parts. First part is Suspicious Region detection and second part is microcalcification detection based on Hessian matrix.

2.1 ROI Detection

In the first stage, Region of Interest (ROI) is detected from the Original mammogram. We proposed the multiresolution based histogram technique for the distinction between microcalcification cluster regions and normal regions in mammograms. The mammogram image was decomposed into four subimages by an undecimated wavelet transform (filter bank implementation without downsampling). The resulting images are one approximation subimage and three detailed subimages. Suspicious areas are found to be mainly concentrated in the detailed subimage. The size of each subimage is the same as the original image. The resulting horizontal detailed subimage or vertical detailed subimage is used to identify the region encircling the microcalcification clusters.

In training set, two different types of square region with size of 30 x 30 were selected from the horizontal detailed subimage. A suspicious region was selected that contains the microcalcification clusters. Normal region was selected randomly that does not contain microcalcification Clusters. We determined histogram of these two types of region. Fig. 1 shows the histogram of suspicious region and Fig. 2 shows the histogram of normal region. The histogram of region with microcalcification clusters has high positive tail and asymmetric. The distribution of right hand tail is larger than left hand tail. The histogram of suspicious region is asymmetric and normal region is symmetric. So the difference between the absolute value of maximum positive coefficient and absolute value of maximum negative coefficient is nearer to zero in normal region. From Fig. 1, it shows that histogram of suspicious region is not Gaussian like distribution. So variance has high value in suspicious region compared to normal region. Region of Interest (ROI) can be identified by using above two properties.

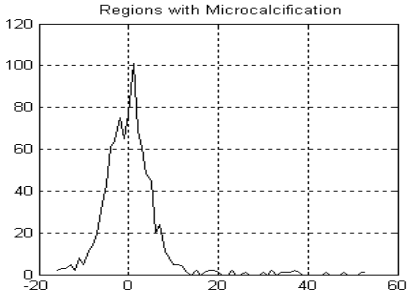

Fig. 1: Histogram of region with microcalcification

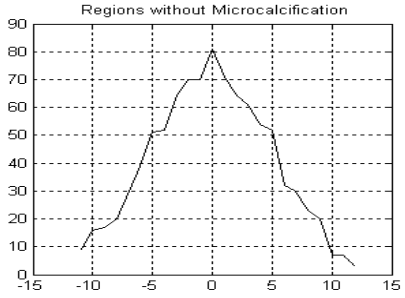

Fig. 2: Histogram of region without microcalcification

Suspicious ROI detection was done as follows. Initially, Mammogram image was decomposed by undecimated wavelet transform. In resulting horizontal detailed subimage was divided into 30 x 30 overlapping square blocks. Difference between the absolute value of maximum positive coefficient (S^{+}_{max}) and maximum negative coefficient (S^{-}_{max}) was calculated at each overlapping region.

$$D^{SR} = \left| S^{+}_{\max} \right| - \left| S^{-}_{\max} \right| \tag{1}$$

$$Var_{SR} = \frac{\sum_{x=i}^{N}\sum_{y=j}^{M}(I_D(x,y) - \tilde{M})^2}{NM} \tag{2}$$

Where, I_D denotes horizontal detail image and $\tilde{M}$ is mean value of each square region of detailed image. D^{SR} denotes Difference value for each square region and Var_{SR} denotes variance of each square region.
Suspicious areas is detected according to following decision rule

$$SR = \begin{cases} 1 & D^{SR} \geq T_1,\ Var^{SR} \geq T_2 \\ 0 & D^{SR} < T_1,\ Var^{SR} < T_2 \end{cases} \tag{3}$$

Where, T_1 and T_2 are thresholds were determined by various experiments. The better ROI selection is obtained while T_1 is set as 5 and T_2 is set as 30.

2.2 Hessian Matrix

After detecting suspicious ROI from mammogram, the next part is to pass an image through a multiscale filter bank, which was designed based on Hessian matrix. The Hessian matrix is a square matrix of second order partial derivates of an arbitrary function [23]. The second order partial derivatives are calculated as intensity difference around the pixel

$$H = \begin{bmatrix} \frac{\partial^2 S}{\partial x^2} & \frac{\partial^2 S}{\partial x \partial y} \\ \frac{\partial^2 S}{\partial y \partial x} & \frac{\partial^2 S}{\partial y^2} \end{bmatrix} \tag{4}$$

$\frac{\partial^2 S}{\partial x^2}$ is second order partial derivative in horizontal direction, $\frac{\partial^2 S}{\partial y^2}$ is second order partial derivative in vertical direction, $\frac{\partial^2 S}{\partial x \partial y}$ is first order partial derivative in horizontal followed by vertical directions and $\frac{\partial^2 S}{\partial y \partial x}$ is first order partial derivative in vertical followed by horizontal directions. Also it is symmetric matrix; the second order partial derivative $\frac{\partial^2 S}{\partial y \partial x}$ is the same as $\frac{\partial^2 S}{\partial x \partial y}$. In filter, image passes through high pass filter in horizontal direction followed by vertical direction is same as

passes through in vertical direction followed by horizontal direction. $\frac{\partial S}{\partial y}$ is computed by applying first order partial derivative in vertical direction and $\frac{\partial S}{\partial x}$ is computed by applying first order partial derivative in horizontal direction.

$$\frac{\partial S}{\partial x} = \frac{1}{2}(z^{-1} - z^{1})^{H} \tag{5}$$

$$\frac{\partial S}{\partial y} = \frac{1}{2}(z^{-1} - z^{1})^{V} \tag{6}$$

H denotes horizontal direction and V denotes vertical direction. Second order partial derivative in horizontal direction was determined by

$$\frac{\partial^2 S}{\partial x^2} = \frac{1}{4}(z^{-2} - 2 - z^{2})^{H} \tag{7}$$

Second order partial derivative in vertical direction was determined by

$$\frac{\partial^2 S}{\partial y^2} = \frac{1}{4}(z^{-2} - 2 - z^{2})^{V} \tag{8}$$

Applying the vertical and horizontal filters successively

$$\frac{\partial^2 S}{\partial x \partial y} = \frac{1}{2}(z^{1} - z^{-1})^{H} \cdot \frac{1}{2}(z^{1} - z^{-1})^{V} = \frac{\partial^2 S}{\partial y \partial x} \tag{9}$$

2.3 Analysis of eigenvalues of Hessian matrix

In order to examine the relation between eigenvalues of Hessian matrix and nodule structure, two sets of data was tested. Fig. 3a shows a microcalcification profile in horizontal direction (Single line on mammogram that contains microcalcification) was taken from mammogram.

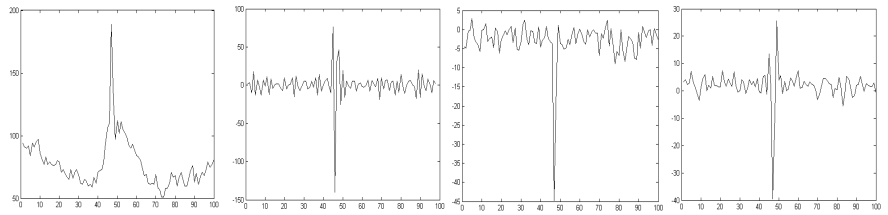

(a) (b) (c) (d)

Fig. 3: Characteristics of microcalcification structure (a) micocalcification profile (b) Second derivative of microcalcification profile (c) First eigen value of Hessian matrix (d) Second eigen value of Hessian matrix

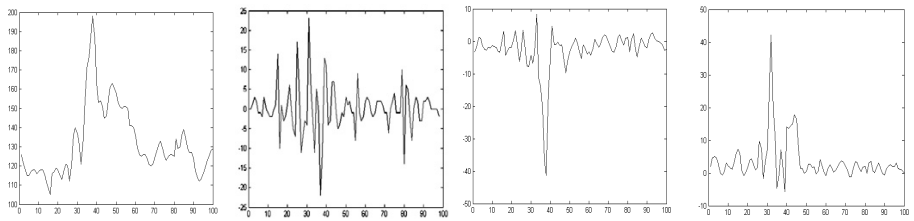

(a) (b) (c) (d)

Fig. 4: Characteristics of Linear structure (a) Linear region profile (b) Second derivative of Linear region profile (c) First eigen value of Hessian matrix (d) Second eigen value of Hessian matrix

Fig. 3b shows second derivative values for Microcalcification profile. Fig. 3c and Fig. 3d shows profile of two eigenvalues of Hessian matrix for microcalcification profile. However, the eigenvalues for microcalcification have large negative values and eigenvalues for background are nearer to zero. Fig. 4a shows a linear region profile of mammogram and Fig. 4b shows second order derivative values. Two eigen value profiles of Hessian matrix are shown in Fig. 4c and Fig. 4d. In two eigen values, one of the eigenvalues has negative value and another one is positive value at sharp linear structure. Eigenvalues are sorted $|\lambda_1| < |\lambda_2|$, small eigen value λ_1 and large eigen value λ_2 are used to extract the desired structures. The eigenvalues of Hessian matrix is able to detect not only microcalcification, also detect blood vessels and mammary ducts. Table 1 summarize the relation between different structure of tissues and eigenvalues of Hessian matrix.

Table 1. Eigenvalues of various structures

λ_1	λ_2	Tissue (regions)
L	L	Background
H^N	H^N	Microcalcification(nodular)
H^P	H^N	Linear structure(blood vessels, mammary ducts), film artifacts
H^N	H^P	
L	H^P (or) H^N	
H^P	H^P	Dark nodule

L indicates low value, H^P and H^N indicates high positive and high negative values. If two eigenvalues are positive high values it indicates dark nodular structure. Generally microcalcification appears in mammogram as bright nodular points. So microcalcification can be detected by following condition

$$\lambda_1 < 0 \; \lambda_2 < 0$$
$$|\lambda_1| \cong |\lambda_2| \tag{10}$$

2.4 Proposed filter Bank based on Hessian matrix

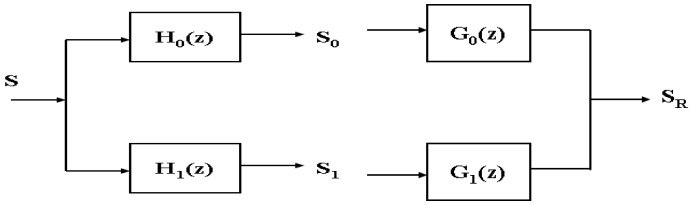

Fig. 5:Two channel analysis and synthesis filter bank

In this chapter, two dimensional filter bank was designed based on Hessian matrix. Fig. 5 shows the one dimensional two channel filter bank of analysis and synthesis bank.
The outputs of the two analysis filters are then

$$S_0(z) = H_0(z)\, S(z) \tag{11}$$

$$S_1(z) = H_1(z)\, S(z) \tag{12}$$

Synthesis filter reconstruction is

$$S_R(z) = G_0(z)\, S_0(z) + G_1(z)\, S_1(z) \tag{13}$$

Substitute Eq.11 & Eq.12 into Eq.13

$$S_R(z) = G_0(z)\, H_0(z)\, S(z) + G_1(z)\, H_1(z)\, S(z)$$
$$= [\, G_0(z)\, H_0(z) + G_1(z)\, H_1(z)\,]\, S(z) \tag{14}$$

At Perfect reconstruction, $S_R(z) = S(z)$

$$G_0(z)\,H_0(z) + G_1(z)\,H_1(z) = 1 \tag{15}$$

From Eq. (5)-(9), $H_0(z)$ is the first order smoothing filter and $H_1(z)$ is the first order derivative filter

$$H_0(z) = \frac{1}{2}(z^{-1} + z^{1}) \tag{16}$$

$$H_1(z) = \frac{1}{2}(z^{-1} - z^{1}) \tag{17}$$

Synthesis filter banks were designed to cancel aliasing and satisfy perfect reconstruction [24]

$$G_0(z) = H_0(z) \tag{18}$$

$$G_1(z) = -H_1(z) \tag{19}$$

So synthesis filter banks was given by

$$G_0(z) = \frac{1}{2}(z^{-1} + z^{1})$$

$$G_1(z) = -\frac{1}{2}(z^{-1} - z^{1}) = \frac{1}{2}(z^{1} - z^{-1}) \tag{20}$$

Second order partial derivative filter was given by

$$H_0(z)G_0(z) = H_0(z)\,H_0(z) = \frac{1}{4}(z^{-2} + 2 + z^{2}) \tag{21}$$

$$H_1(z)G_1(z) = -H_1(z)\,H_1(z) = -\frac{1}{4}(z^{-2} - 2 + z^{2}) \tag{22}$$

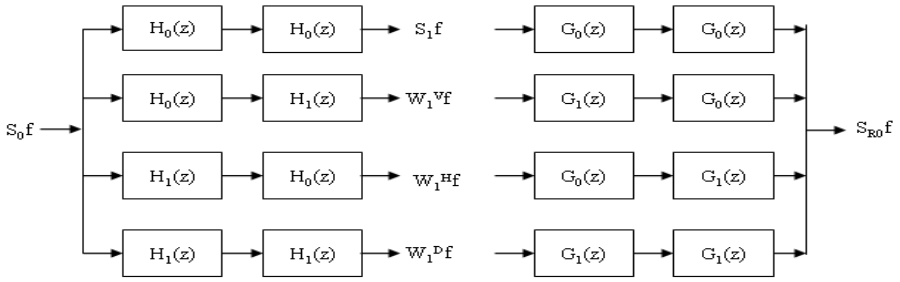

Fig. 6: Two dimensional filter bank

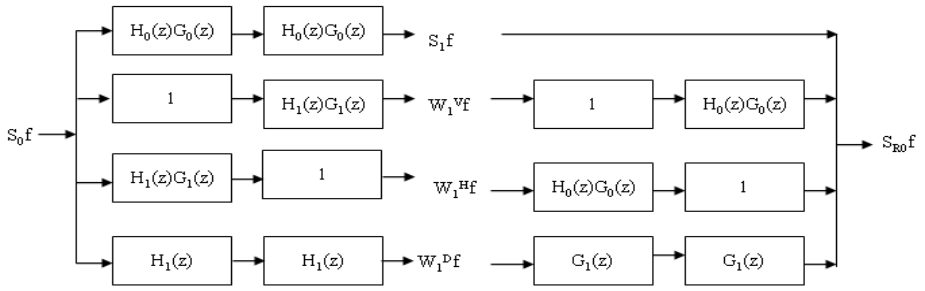

Fig. 7: Alteration of two dimensional filter bank for calculating Hessian matrix

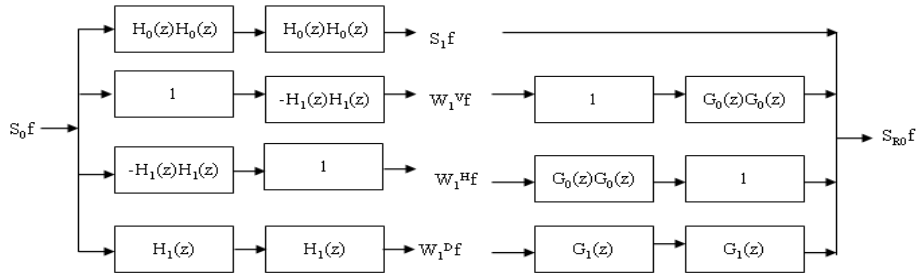

Fig. 8: Filter bank designed based on Hessian matrix which is equivalent to Fig. 7

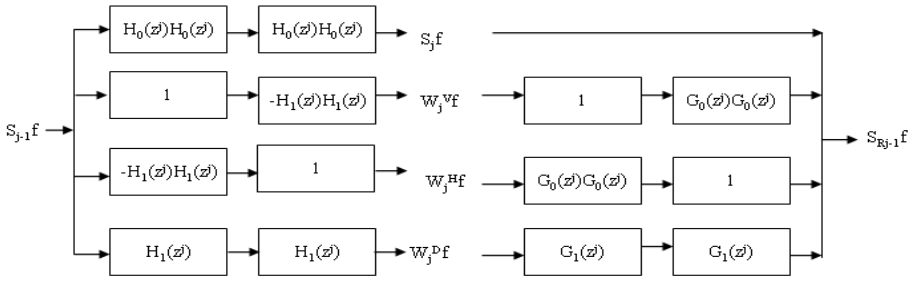

Fig. 9: Hessian matrix filter bank with iterating low pass image

Fig. 6 shows the two dimensional filter bank. Some of the filters were moved from synthesis to analysis and vice versa to determine the Hessian matrix. So Fig. 6 changed into Fig. 7, which is used to calculate Hessian matrix. Substitute Eq. (16)-(22) into Fig.7, it changed into Fig. 8, which is equivalent to Fig. 7. The multiscale image analysis was achieved by approximation subimage $S_j f$ was iterated to number of scales. Image was smoothed and dilutes the noise at each scale. Filter $H_0(z^j)$ and $H_1(z^j)$ is 2j scale dilation of $H_0(z)$ and $H_1(z)$. Coefficients of filter at higher scale is obtained by putting 2^j-1 zeros between each of the coefficient of first scale filter coefficients. $\frac{\partial^2 S}{\partial x^2}$, $\frac{\partial^2 S}{\partial y^2}$, $\frac{\partial^2 S}{\partial x \partial y}$ are corresponds to W_j^V, W_j^H and W_j^D. Generally the microcalcifications are high-frequency components; microcalcification detection is achieved by decomposing the mammogram into different frequency subbands, suppressing the lowest frequency subband, and reconstructing only the high frequency subbands. But reconstructed image contains not only microcalcification also it have some undesirable structural elements which is high frequency in nature. In our proposed method, subbands containing high frequencies which are only nodular structure are reconstructed by introducing Hessian matrix concepts

Hessian matrix was calculated at each coefficient of each scale. So Hessian matrix was given by

$$\mathrm{H} = \begin{bmatrix} W_j^V & W_j^D \\ W_j^D & W_j^H \end{bmatrix} \tag{23}$$

$$\lambda_1, \lambda_2 = \text{Eigen value (H)} \tag{24}$$

$$W_j^M(x,y) = \begin{cases} W_j^M(x,y) & \lambda_1 < TH_1, \lambda_2 < TH_2 \\ 0 & otherwise \end{cases} \tag{25}$$

Here M represents all high frequency subbands (vertical, horizontal and diagonal), x and y indicates each coefficient value. Mammogram image was decomposed upto n scale, lowest frequency subband S_n is suppressed and all high frequency subbands are reconstructed. The coefficients of detail planes are thresholded to zero if their eigenvalues of Hessian matrix are greater than preset threshold else kept unchanged. The remaining significant coefficients are recovered which gives microcalcification detected image. TH_1 and TH_2 are negative thresholds which were determined by trial run.

3. Result & Discussion

We have tested our proposed method in MATLAB 7.0 and mammogram images were taken from DDSM database which contains left and right breast images for 100 patients and consists of 200 images obtained both craniocaudal (CC) and the mediolateral oblique (MLO) projection view. The mammograms were originally of size 1770×2370 with the pixel resolution (100 um/pixel). The DDSM databases are classified according to its features and radiologists interpretation.The first step of microcalcification detection was to find the suspicious regions. These regions are identified by multiresolution based histogram technique described on section 2.1. Fig. 10a and Fig. 10c shows a part of mammogram image with microcalcification clusters. Fig. 10b and Fig. 10d shows suspicious areas are marked by 1(white) and other regions are marked by 0(black).

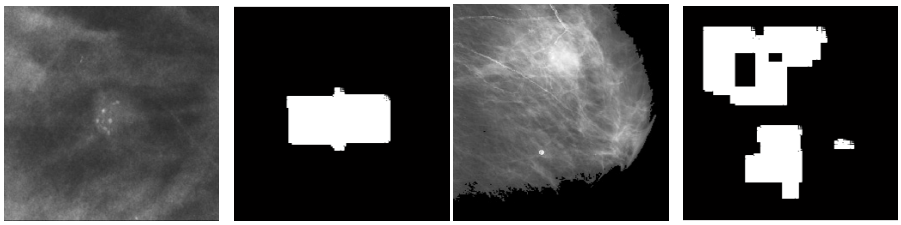

Fig. 10: ROI detection (a),(c) Mammogram with microcalcification clusters (b),(d) suspicious ROI detection

A 100 x 100 square area was chosen as ROI size which is enough to cover the microcalcification. The square matrix was moved on suspicious areas (marked by white) horizontally and vertically in ten pixel displacement. Each square area was considered as suspicious ROI and this ROI was extracted from Original mammogram image. Sometimes normal regions which appear similar to the suspicious regions are marked as suspicious ROI. Also these regions don't contain microcalcification clusters. But filter bank based on Hessian matrix can detect the True regions and reduces false positive rate.
Fig. 11a shows the Region which contains nodular components (microcalcification) and Fig. 12a shows a region which contains linear components. Fig. 11, 12 (b to f) shows the subimages at scales from 1 to 5. At first scale more number of coefficients has negative eigenvalues because first scale is more sensitive to noise shown in Fig. 11b, Fig. 12b. From scale 2 images are smoothed at each scale by smoothing filter. Nodular components of different sizes can be detected accurately by using filter bank based on Hessian matrix.

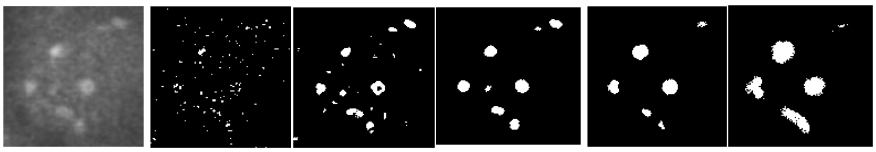

Fig. 11: Nodular detection on suspicious ROI (a) Original Suspicious ROI (b)-(f) subimages upto 5 scale

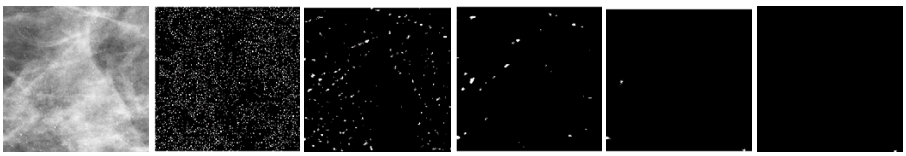

Fig. 12 : Nodular detection on normal ROI (a) Original Normal ROI (b)-(f) subimages upto 5 scale

The large eigenvalue which is less than Threshold T(We set -5) were calculated at each scale and plotted. Fig. 13 shows the cumulative plot was obtained from average value of large eigenvalue which is less than Threshold T. The cumulative value was calculated from 50 suspicious ROI (Region with microcalcification) and 50 normal ROI (regions without microcalcifications).

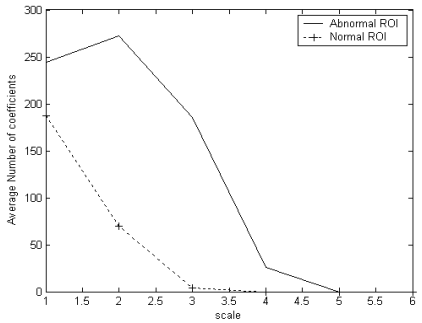

Fig. 13: Comparison of Suspicious ROI with Normal ROI of different scales

The value was decreased from scale 2 to 5 and the maximum value indicates the size of microcalcification equivalent to width of the filter. Also it implies that most of eigenvalues at scale 5 are zero. So filter bank upto scale 4 which is used to detect microcalcification in mammogram. The low-pass(smoothing) image are iterated upto 4 scales, the lowest subimage of scale 4 are suppressed and reconstructed the high frequency subbands which contains only nodular components. Also it shows large eigenvalues less than Threshold T is towards zero at scale 1 to 4 for linear and normal regions.

The performance of proposed method on mammogram images were compared with background suppressed algorithm. For convenience, we compared microcalcification detection by 2D wavelet transform [12] and multiscale wavelet method (trous wavelet transform) [19]. Fig. 14a shows a region which contains microcalcification clusters (suspicious ROI) of size is 100x100. Fig. 14(b)-(d) shows microcalcification detection by 2D wavelet, multiscale wavelet and proposed method. From the results it shows nodular components (microcalcification) were accurately extracted from suspicious ROI by proposed method. Linear components and some of the artifacts which are high frequency in nature are also extracted by other two methods. An experiment on another mammogram is illustrated in Fig 15. The results showed in Fig. 15b and Fig. 15c appear to be veiled by the unwanted artifacts compared to Fig.15d.

A statistical evaluation of the experimental results obtained by various detection methods in connection with the labeling of the expert radiologist was analyzed. Free response operating characteristic (FROC) is the curve to evaluate the performance of microcalcification detection methods. The FROC curve is a plot of the True positive ratio (TP) versus the false positive (FP) numbers per an image. An FROC curve presents a summary of the percentage of suspicious regions truly detected (sensitivity) and the percentage of normal regions labeled correctly (specificity). The TP ratio is true observation ratio, which shows how many microcalcifications are truly detected.

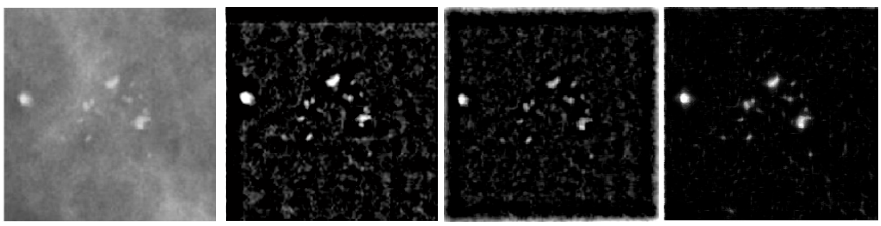

Fig. 14 : Detection of microcalcification (a) Original Suspicious ROI (b) Detection by 2D WT (c) Detection by Multiscale WT (d) Detection by Proposed Method

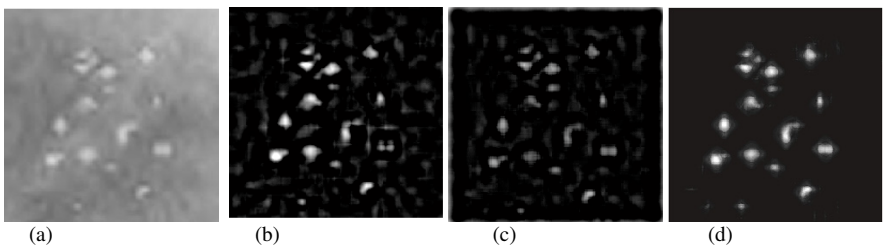

Fig. 15 : Detection of microcalcification (a) Original Suspicious ROI (b) Detection by 2D WT (c) Detection by Multiscale WT (d) Detection by Proposed Method

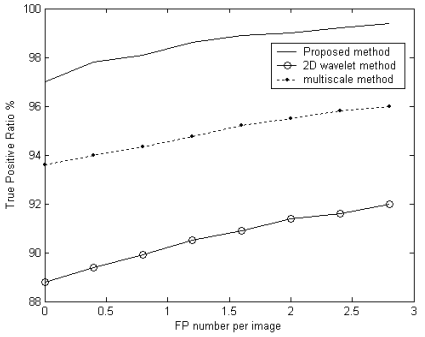

Fig. 16 : Comparison of FROC curve for detection of Microcalcification clusters

from suspicious regions; and the False positive number/image refers to a normal region is wrongly identified as abnormality. In the FROC curve as shown in Fig. 16, three microcalcification detection methods were compared.
One is our proposed method, and the others two are detection method based on 2D wavelet and multiscale wavelet method. The FROC test was conducted on 100 images taken from DDSM database. We obtained 98.3% TP ratio with 0.9 FP numbers/image for proposed method. The TP ratio of 2D wavelet method is 89.5% for a 0.75 FP number/image and in multiscale wavelet method, the TP ratio is 94.35 % for 0.8 FP numbers/image. Fig. 16 shows that the proposed method has high TP ratio compared to other two methods.

4. Conclusion

This paper proposed microcalcification detection by novel filter bank, which was designed based on Hessian matrix. In many conventional methods, detection of microcalcifications is achieved by suppressing lowest subband and reconstructing all high frequency subbands. In our proposed scheme, reconstructing the high frequencies contains only nodular components. This method is better to differentiate the microcalcification clusters from insignificant tissues. Experimental Results show that the proposed method achieves high TP ratio compared with conventional microcalcification detection methods. In the future, we aim to apply our method to compute the size of each microcalcification and find out a better way to calculate the threshold automatically.

Acknowledgements

The authors would like to thank Dr. Murugesan, Radiologist, Johnsons MRI Scan Centre & Diagnostic Centre**,** Erode for providing us with sufficient data and his valuable advice. The authors also thank to Dr.K. Govindaraj, Director, GVN Cancer Cure Centre & GVN Institute of Medical Sciences, Trichy for his help.

References

[1] Heath, M., Bowyer, K., Kopans, D., Moore, R., Kegelmeyer, P . The digital database for screening mammography. In: Proceedings of the 5th International Workshop on Digital Mammography. Medical Physics Publishing(Madison,WI), pp.662–671,2000

[2] C. J. Vyborny and R. A. Schmidt. Technical image quality and the visibility of mammographic detail, in Syllabus: A Categorical Course in Physics-Technical Aspects of Breast Imaging, A. G. Haus and M. J. Yaffe, Eds. Oak Book III: Radiological Society of North America, pp.103–111, 1994

[3] G. M. te Brake and N. Karssemeijer .Single and multiscale detection of masses in digital mammograms.*IEEE Trans. Medical Imaging*, vol. 18, no. 7, pp. 628–639, July 1999

[4] R. G. Bird, T. W. Wallace, and B. C. Yankaskas .Analysis of cancers missed at screening mammography. *Radiology*,vol. 184, pp. 613–617,1992.

[5] M. L. Giger, P. Lu, Z. Huo, U. Bick, C. J. Vyborny, R. A. Schmidt, W. Zheng, C. E. Metz, D. Wolverton, R. M.Nishikawa, W. Zouras, and K. Doi .CAD in digital mammography: Computerized detection and classification of masses. in *Digital Mammography*, A. G. Gale, Ed. *Et al.* Amsterdam/New York: Elsevier Science, pp. 281–287,1994

[6] W. P. Kegelmeyer, Jr, J. Prundeda, P. Bourland, A. Hillis, M. Riggs, and M.Nipper . Computer aided mammographic screening for Speculated lesions.*Radiology*, vol. 191, pp. 331–337, 1994

[7] K. Doi, H. MacMahon, S. Katsuragawa, R. M. Nishikawa, and Y. Jiang . Computer-aided diagnosis in radiology: Potential and pitfall. *Eur. J. Radiol.*, vol. 31, pp. 97–109,1999

[8] H. Li, K. J. Liu, and S. Lo . Fractal modeling and segmentation for the enhancement of microcalcifications in digital mammograms. *IEEE Trans.Med.*

Imag., vol. 16, no. 6, pp. 785–798, December 1997

[9] S. Yu, L. Guan .A CAD system for the automatic detection of clustered microcalcifications in digitized mammogram films", *IEEE Trans. .Med. Imag*., vol. 19, no.2, pp. 115–126,1998

[10] S.Mallat . A compact multiresolution representation: the wavelet model. *Proc. IEEE Computer Society Workshop on Computer Vision,* IEEE Computer Society Press, Washington, D.C., p.2-7.1987

[11] S. Mallat .Multifrequency channel decompositions of images and wavelet models*, IEEE Trans. Acoust. Speech Signal Process.*, vol. 37, no. 12, pp. 2091–2110, December 1989

[12] Ted C. Wang and Nicolaos B. Karayiannis .Detection of Microcalcifications in Digital Mammograms Using Wavelets. *IEEE Tran. on Medical Imaging*, vol. 17, pp. 498-509,August 1998

[13] R. N. Strickland and H. I. Hahn . Wavelet transform for detecting microcalcifications in mammograms. *IEEE Trans. Med. Imag*., vol. 15, no. 2, pp. 218–229, April 1996

[14] H. Yoshida, K. Doi, and R. M. Nishikawa.Automated detection of clustered Microcalcifications. *Proc. SPIE (Digital Mammograms using Wavelet Transform Tech., Med. Imag. 1994: Image Process.)*, vol. 2167, pp. 868–886, February 1994

[15] H. Yoshida, K. Doi, R. M. Nishikawa, M. L. Giger, and R. A. Schmidt. An improved computer-assisted diagnostic scheme using wavelet transform for detecting clustered microcalcifications in digital mammograms. *Acad. Radiol*., vol. 3, pp. 621–627. 1996

[16] Damir Sersic and Sven Loncaric..Enhancement of Mammographic Images for Detection of Microcalcifications. Fac. of Electrical Engineering and Computing, Zagreb, Croatia. 1998

[17] A.F. Laine, S. Schuler, J. Fan, and W. Huda. Mammographic feature enhancement by multiscale analysis. *IEEE Trans. Med. Imag.*, vol. 13,no. 4, pp. 725–740, December 1994

[18] F. Laine, J. Fan, andW. Yang.Wavelets for contrast enhancement of digital mammography. *IEEE Eng. Med. Biol. Mag*.,vol. 14, no.5, pp. 536–550, September – October 1995

[19] Chun-Ming Chang and Andrew Laine. Coherence Of Multiscale Features for Enhancement of Digital Mammograms. *IEEE Tran. on Information Technology in Biomedical*, vol. 3, pp. 32-46, 1999

[20] Y. Sato, C.-F. Westin, A. Bhalerao, S. Nakajima,N.Shiraga, S. Yoshida, and R. Kikinis .Tissue classification based on 3D local intensity structures for volume rendering. *IEEE Transactions on Visualization and Computer Graphics*, 6(2):160–180,2000

[21] Frangi, W. Niessen, K. Vincken, and M. Viergever . Multiscale vessel enhancement filtering. *Medical Image Computing and Computer - Assisted Intervention – MICCAI'98*,(1496):130–137,1998

[22] 22. K. Krissian, G. Malandain, N. Ayache, R. Vaillant, and Y.Trousset . Model based detection of tubular structures in 3D images. *Comp. Vision and Image Understanding*, vol. 80, no. 2, pp. 130-171, November 2000

[23] Sato Yoshinobu, et al.: *3D Multi-Scale Line Filter for Segmentation and Visualization of Curvilinear Structures in Medical Images*,in proc. of the First Joint Conference on Computer Vision, Virtual Reality and Robotics in Medicine and Medial Robotics and Computer-Assisted Surgery, volume 1205 of Lecture Notes in Computer Science, pages 213– 222, March 1997

[24] D.Esteban, C.Galand : *Application of Quadrature mirror filter to split Band Voice Coding Schemes*. Proc. IEEE ICASSP'77,pp.191-195, May 1977.